USP21 Deubiquitinase Elevates Macropinocytosis to Enable Oncogenic KRAS Bypass in Pancreatic Cancer

Pingping Hou, Xingdi Ma, Zecheng Yang, Qiang Zhang, Chang-Jiun Wu, Jun Li, Lin Tan, Wantong Yao, Liang Yan, Xin Zhou, Alec C. Kimmelman, Philip L Lorenzi, Jianhua Zhang, Shan Jiang, Denise Spring, Y. Alan Wang, and Ronald A. DePinho

Supplemental Figures S1-8

Supplemental Table S1-2

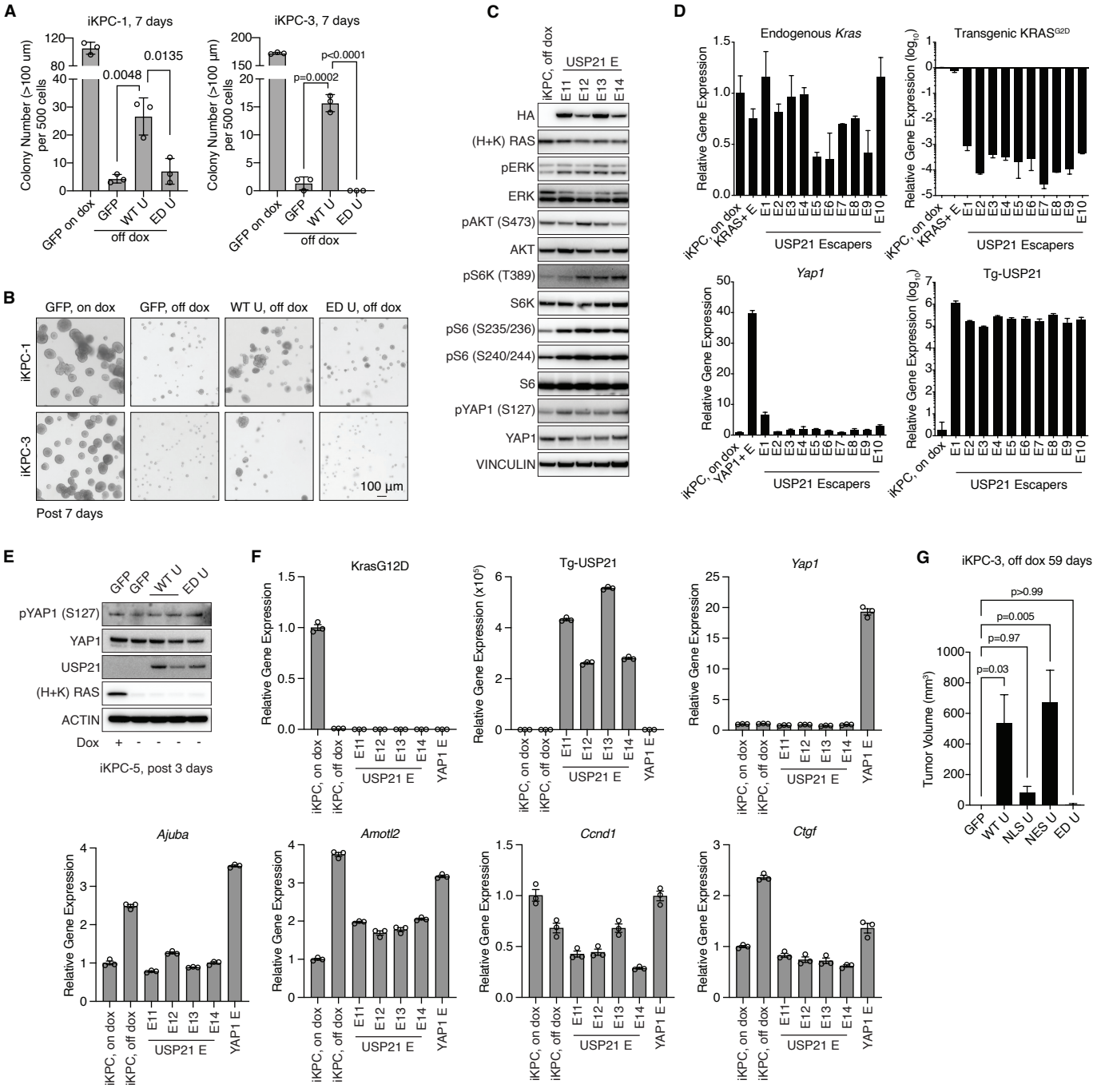

Figure S1. USP21 promotes the bypass of KRAS* dependency in PDAC. (A-B) KRAS*-independent colony formation analysis. (**A**) and representative images (**B**) comparing GFP-, WT USP21- and ED USP21-OE iKPC cells. GFP-OE iKPC cells w/ dox is positive control. (**C**) Western blot analysis of KRAS* signaling pathway and YAP1 in USP21 escaper cells. KRAS*-extinguished iKPC cells are control. (**D**) Validation of gene expression of endogenous Kras, transgenic KrasG12D, Yap1, and exogeneous USP21 by RT-PCR. Data are represented as mean ± SD. (**E**) Western blot analysis of YAP1 phosphorylation in GFP-, WT U- and ED U-OE iKPC cells after KRAS* extinction for 3 days. KRAS*-expressing cells are control. (**F**) Expression of canonical YAP1 target genes in USP21 escapers. Dox on and off iKPC cells and *de novo* generated YAP1 amplified escaper cells (YAP1 E) are control samples. (**G**) KRAS*-independent colony formation analysis comparing GFP-, WT USP21-, nucleus-localized NLS USP21-, cytoplasm-localized NES USP21- and ED USP21-OE iKPC cells. For A and F, data are represented as mean ± SEM. E1-E14, USP21 escapers.

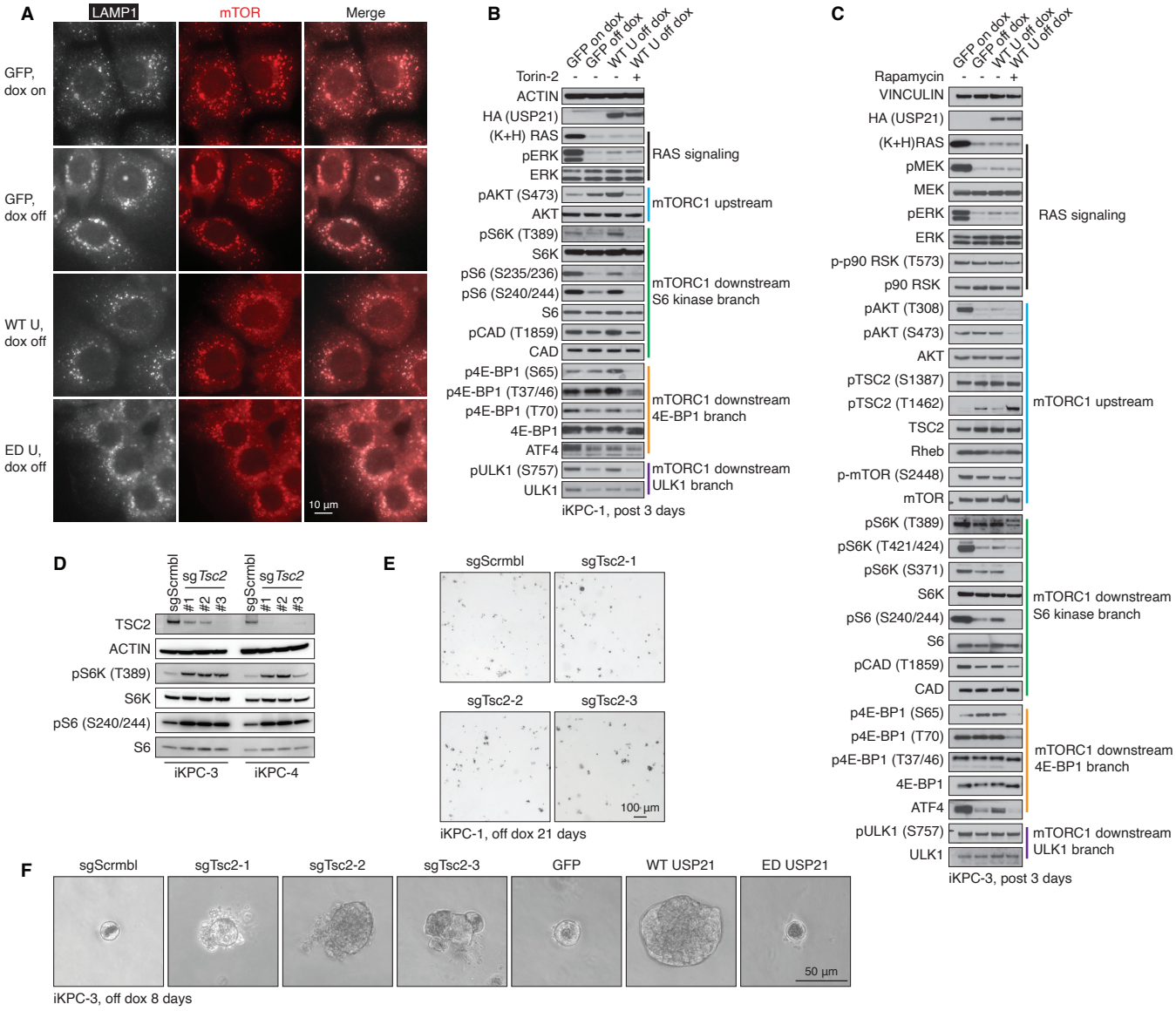

Figure S2. USP21 does not regulate mTOR localization or upstream signaling activation. (**A**) Immunofluorescence staining of mTOR and LAMP1 in GFP-, WT USP21- and ED USP21-OE iKPC cells at day 3 after KRAS* extinction. KRAS*-expressing GFP-OE iKPC cells are positive control. (**B-C**) Western blot analysis comparing WT USP21-OE iKPC cells treated with DMSO and mTOR inhibitor Torin-2 (B) or rapamycin (C). (**D**) Validation of sgRNAs targeting Tsc2 by western blot analysis. (**E**) KRAS*-independent colony formation analysis comparing scramble control and Tsc2 sgRNAs in iKPC cells. (**F**) Colony morphology comparison between iKPC cells overexpressing Tsc2 sgRNAs and USP21 variants.

Supplemental_Fig_S3

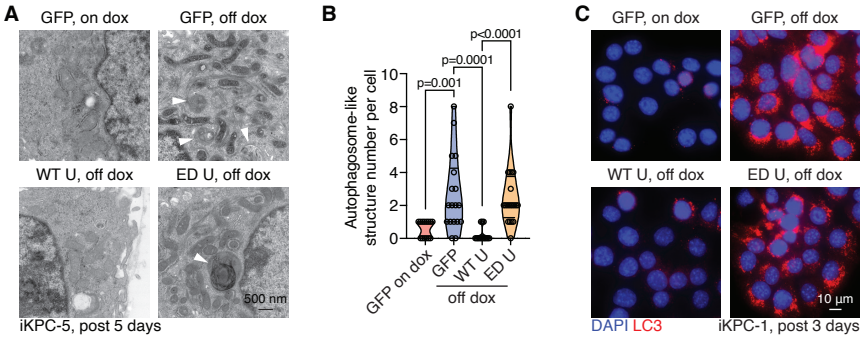

Figure S3. USP21 relieves KRAS*-extinction induced metabolic stress. (**A-B**) Representative TEM images (A) and autophagosome quantification (B) comparing GFP-, WT USP21- and ED USP21-OE iKPC cells at day 5 after KRAS* extinction. GFP-OE iKPC cells w/ dox is positive control. Autophagosome structures were indicated by white arrowheads. Data are represented as mean ± SEM. (**C**) Representative LC3 staining comparing GFP-, WT USP21- and ED USP21-OE iKPC cells at day 3 after KRAS* extinction. GFP-OE iKPC cells w/ dox is positive control.

Supplemental_Fig_S4

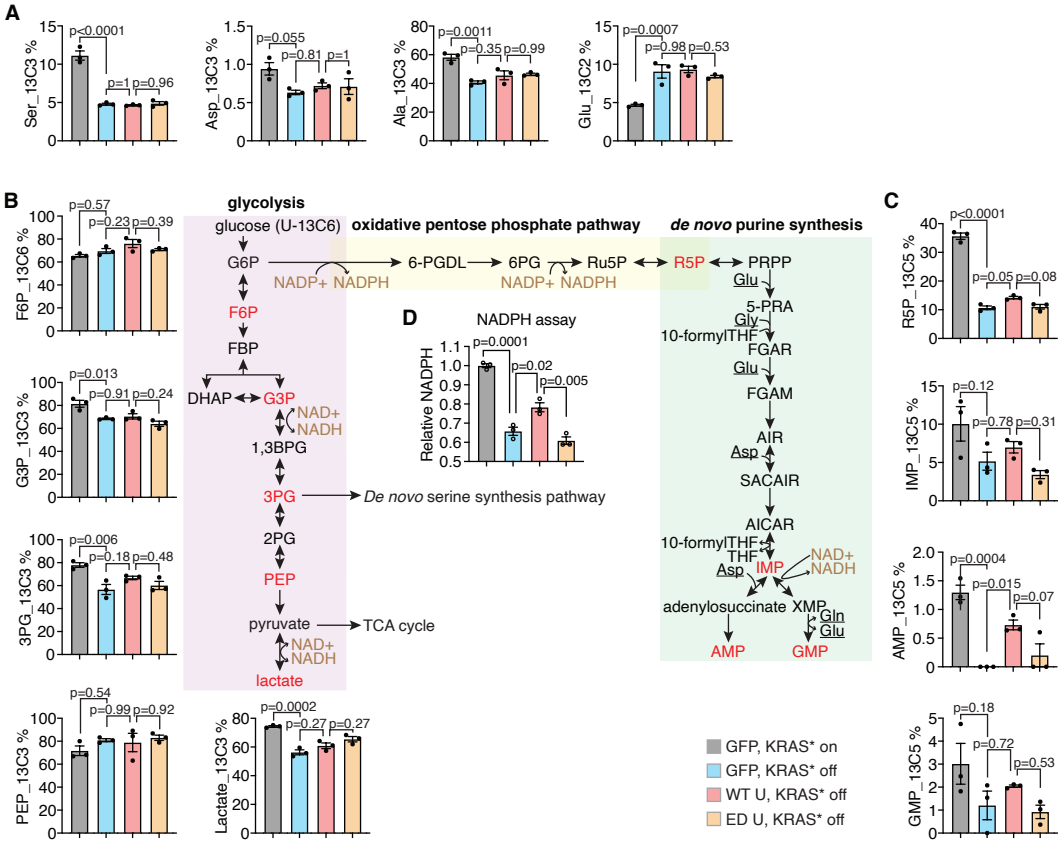

Figure S4. USP21 does not promote metabolic flux to the de novo amino acid synthesis pathways. (**A-C**) Metabolic flux analysis of KRAS*-on GFP-OE iKPC cells and KRAS*-off GFP-, WT USP21- and ED USP21-OE iKPC cells using isotope labeled glucose. Samples were pulse labeled for 15 minutes before collection. Comparison of selected metabolites in amino acid synthesis pathways (A), glycolysis (B) and *de novo* purine synthesis pathway (C) are shown. (**D**) NADPH quantification assay comparing KRAS*-on GFP-OE iKPC cells and KRAS*-off GFP-, WT USP21- and ED USP21-OE iKPC cells. For A-D, data are represented as mean ± SEM.

Supplemental_Fig_S5

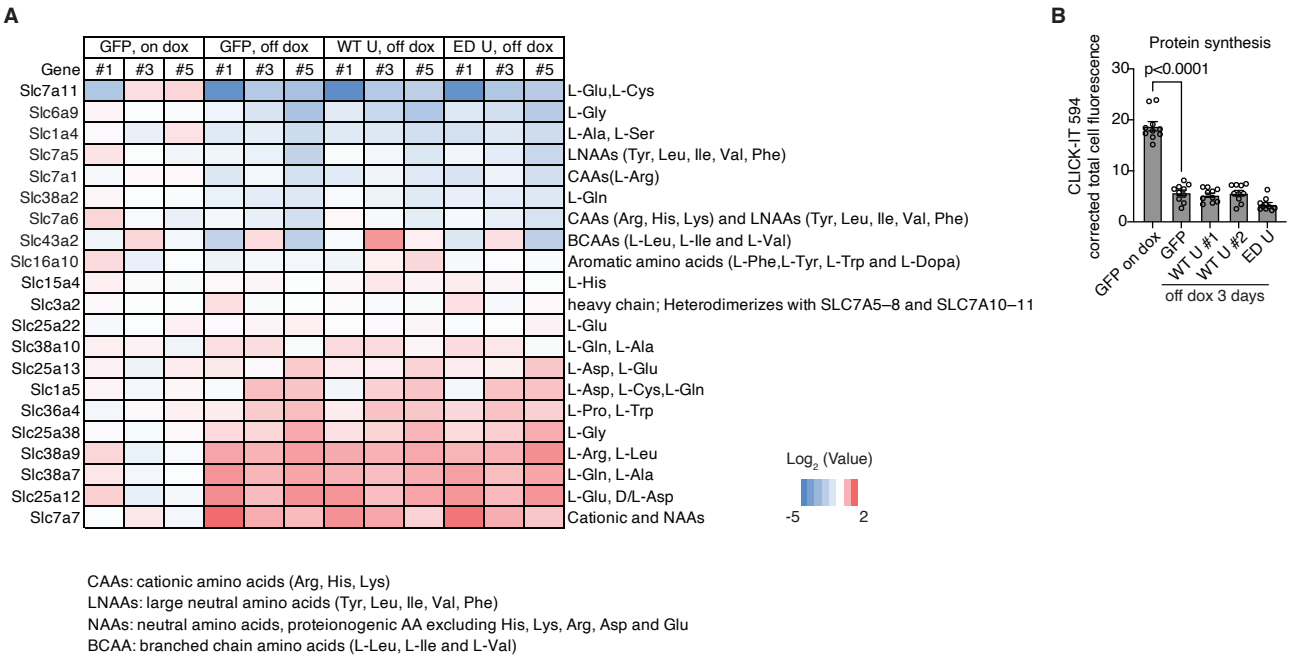

Figure S5. USP21 does not alter amino acid transporter expression pattern at transcriptional level. (**A**) Relative gene expression to KRAS*-on GFP-OE iKPC cells were calculated using RPKM values from RNA sequencing data. The #1, #3 and #5 were three independent iKPC cell lines. The KRAS*-on GFP-OE iKPC cells and KRAS*-off GFP-, WT USP21- and ED USP21-OE iKPC cells were compared. (**B**) Protein synthesis analysis comparing KRAS*-on GFP-OE iKPC cells and KRAS*-off GFP-, WT USP21- and ED USP21-OE iKPC-5 cells. Data are represented as mean ± SEM.

Supplemental_Fig_S6

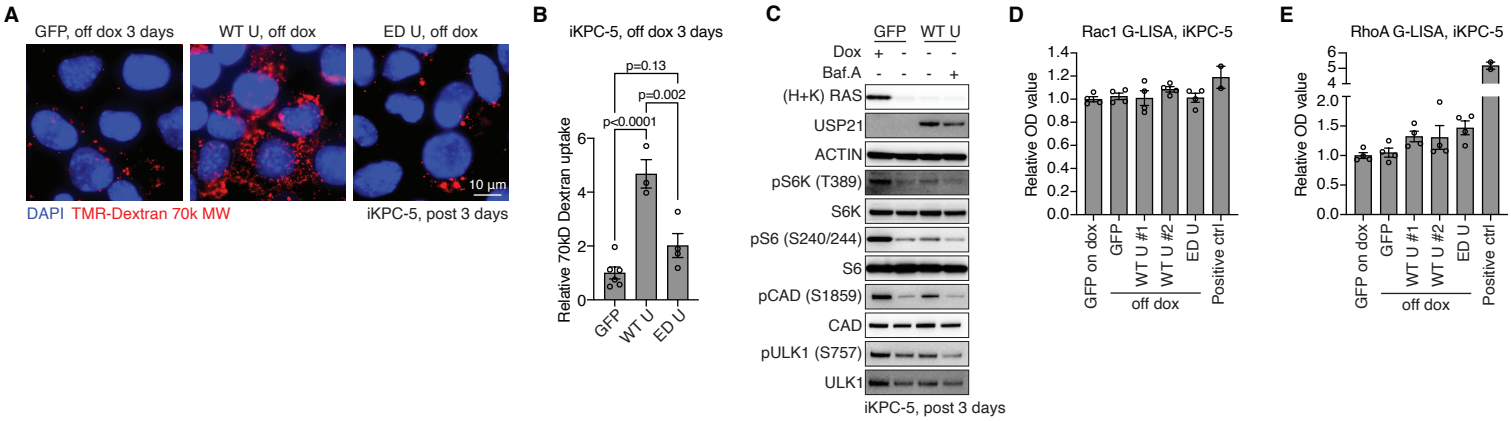

Figure S6. USP21 elevates macropinocytosis activity after KRAS* extinction. (**A-B**) Representative images (A) and the quantification of Dextran particle uptake (B) comparing GFP-, WT USP21- and ED USP21-OE iKPC cells at day 3 after KRAS* extinction. (**C**) Inhibition of macropinocytosis suppresses mTOR activation by USP21. WT USP21-OE iKPC-5 cells with and without bafilomycin A (Baf.A) treatment were collected 3 days after KRAS* extinction for western blot analysis. GFP-OE iKPC cells w/ dox is positive control; GFP-OE iKPC cells w/ o dox is negative control. Baf.A was added 24 hours before collection at 100nM. (**D-E**) G-LISA analysis of Rac1 (C) and RhoA (D) activity comparing KRAS*-on GFP-OE iKPC cells and KRAS*-off GFP-, WT USP21- and ED USP21-OE iKPC cells. Rac1 and RhoA proteins are positive controls, respectively. For B-D, data are represented as mean ± SEM.

Supplemental_Fig_S7

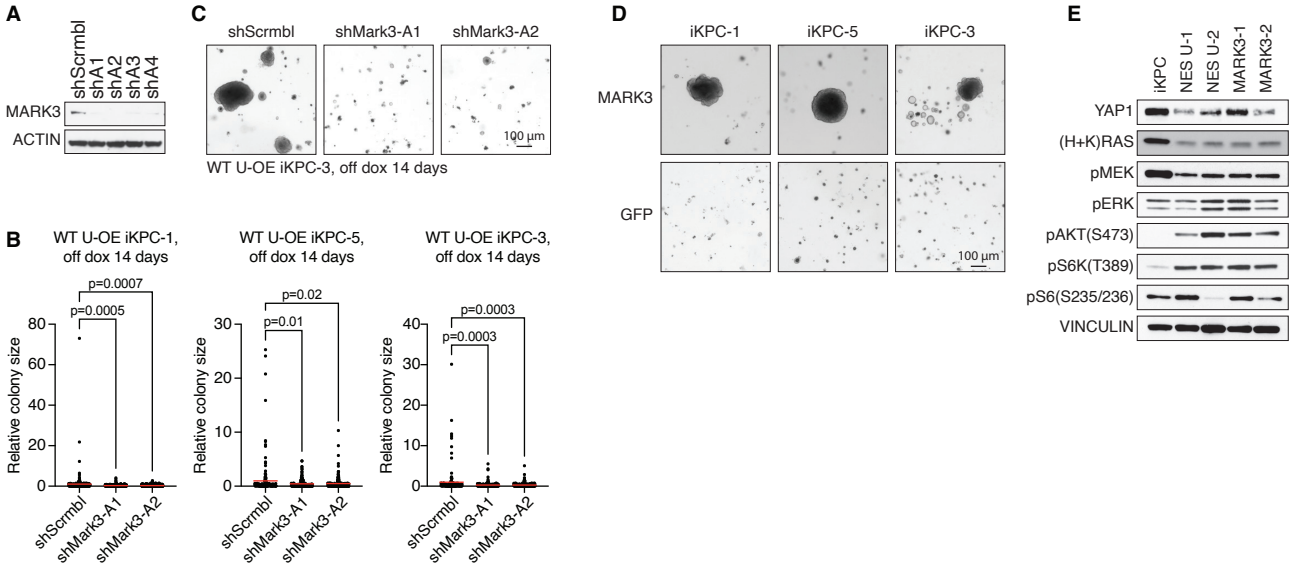

Figure S7. MARK3 is required for USP21-driven KRAS* bypass. (**A**) Western blot analysis of MARK3 protein level after gene knockdown. (**B-C**) KRAS*-independent colony formation analysis (B) and representative images (C) comparing scramble control and Mark3 knockdown in WT USP21-OE iKPC cells after KRAS* extinction. (**D**) Representative images of colonies comparing GFP- and MARK3-OE iKPC cells after KRAS* extinction. (**E**) Western blot analysis of KRAS downstream signaling pathways in parental iKPC cells, NES USP21 escaper cells and MARK3 escaper cells.

Supplemental_Fig_S8

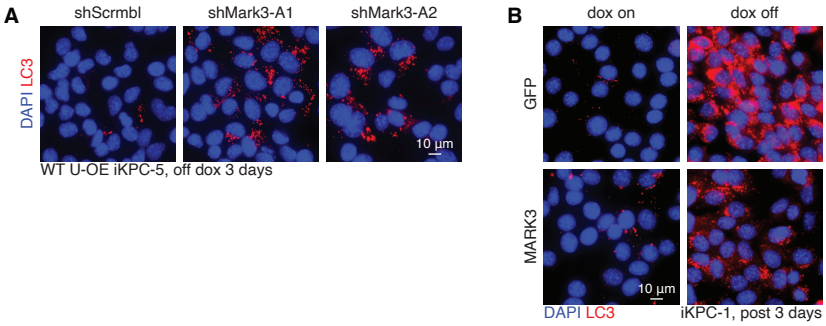

Figure S8. MARK3 regulates autophagy. (**A**) Representative images of LC3 staining comparing WT USP21-OE iKPC cells with scramble control and Mark3 shRNAs at day 3 after KRAS* extinction. (**B**) Representative images of LC3 staining comparing GFP- and MARK3-OE iKPC cells at day 3 after KRAS* extinction.

Supplemental_Table_S1

ID	Gene ID	Sequence
shMark3-A1	NM_022801	CCGGCGGGAAGTACAGAATCCCTTTCTCGAGAAAGGGATTCTGTACTTCCCGTTTTT
shMark3-A2	NM_022801	CCGGCGGAAACTACAGACTGTTGAACTCGAGTTCAACAGTCTGTAGTTTCCGTTTTT
shMark3-A3	NM_022801	CCGGGCTAAGTTTAGACAGATTGTTCTCGAGAACAATCTGTCTAAACTTAGCTTTTT
shMark3-A4	NM_022801	CCGGGAGTAATATTTAGGCAATAACCTCGAGGTTATTGCCTAAATATTACTCTTTTTG
sgTsc2-1	NM_011647.2	GACTGAGTTTATCATCACAT (targeted sequence)
sgTsc2-2	NM_011647.2	TCATTCGGATGCGATTGTTG (targeted sequence)
sgTsc2-3	NM_011647.2	CTCACCTGTCCTCCATGATG (targeted sequence)

Supplemental_Table_S2

Antibody	Application	Vendor	Cat. #
USP21	IHC	Sigma	HPA028397
USP21	WB	Santa Cruz	sc-79305
FLAG	IP, WB	Sigma	F1804
HA	IP, WB	BioLegend	901501
ubH2A	WB	CST	8240
YAP1	IHC, WB	CST	14074
Ki67	IHC	Thermo	RM-9106-S1
total RAS (H+K)	WB	abcam	ab191595
pMEK	WB	CST	4694
MEK	WB	CST	9154
pERK	IHC, WB	CST	4370
ERK	WB	CST	4695
pAKT (S473)	WB	CST	4060
AKT	WB	CST	2920
pS6K (T389)	WB	CST	9234
S6K	WB	CST	2708
pS6 (S235/236)	IHC, WB	CST	4858
pS6 (S240/244)	WB	CST	2215
S6	WB	CST	2217
pULK1 (S757)	WB	CST	14202
ULK1	WB	CST	8054
LC3	IF	CST	83506
LAMP1	IF	Santa Cruz	sc-19992
mTOR	IF	CST	2983
pCAD (T1859)	WB	CST	12662
CAD	WB	CST	93925
p4E-BP1 (S65)	WB	CST	9451
p4E-BP1 (T37/46)	WB	CST	2855
p4E-BP1 (T70)	WB	CST	9455
4E-BP1	WB	CST	9452
ATF4	WB	CST	11815
TSC2	WB	CST	4308
MARK3	WB	abcam	ab52626
ACTIN	WB	Sigma	A2228
VINCULIN	WB	Sigma	V4505
Anti-rabbit IgG, HRP-linked	WB	CST	7074s
Anti-mouse IgG, HRP-linked	WB	CST	7076s
Rabbit anti-Goat IgG (H+L)	WB	Thermo	61-1620